Molecular Cell, Volume *30*

Supplemental Data

The RNA Polymerase II Trigger Loop Functions in Substrate Selection and Is Directly Targeted by α-amanitin

Craig D. Kaplan, Karl-Magnus Larsson, and Roger D. Kornberg

Table S1

Polymerase	Max Elongation Rate (k_{cat})(nt/s)	[Substrate$_{0.5}$] (K_M)(μM)	k_{cat}/K_M	Mutant/WT (ratio of Mutant (k_{cat}/K_M)/ WT (k_{cat}/K_M))	Selectivity for NTPs (k_{cat}/K_M NTPs)/ (k_{cat}/K_M 2'-dNTP)
	NTPs				
WT	11.8±2.9	70±30	0.17	-	
H1085Y	1.4±0.6	110±70	0.01	0.07	
F1084I	16.6±4.0	130±40	0.12	0.71	
F1086S	5.0±0.3	30±3	0.15	0.85	
E1103G	39.0±8.1	140±30	0.28	1.62	
Calf Thymus Pol II	2.4±1.0	290±130	0.01	NA	
	2'-dGTP				
WT	0.026±0.002	50±10	0.0005	-	325×
H1085Y	0.009±0.001	40±10	0.0002	0.41	58×
F1084I	0.054±0.013	60±3	0.0009	1.59	145×
F1086S	0.008±0.001	40±10	0.0002	0.36	760×

E1103G	0.150±0.019	80±10	0.0019	3.51	150X
Calf thymus Pol II	0.002±0.0002	20±2	0.0001	NA	59X
	2'-dATP				
WT	0.006±0.0009	160±40	0.00003	-	5034X
H1085Y	0.002±0.0007	120±60	0.00002	0.59	617X

Maximum elongation rate in nucleotides/second shown with ± indicating the extent of the 95% confidence interval as determined by curve-fitting of plotted data by non-linear regression using GraphPad Prism. K_M values determined from same curve-fitting and shown with ± standard error, as determined in GraphPad Prism. The standard errors are quite large for these determinations, but are in line with those reported by (Vassylyev et al., 2007), and the determinations must be considered only approximate.

Table S2

Polymerase	**K_i α-amanitin (μg/mL)**
	From transcription of 51 nts
WT	300±60
H1085Y	67±36
F1084I	880±210
E1103G	870±120
	From transcription of 13 nts
WT	250±30
F1086S	6±1

K_i values of α-amanitin inhibition of WT and mutant Pol II enzymes determined by curve-fitting the inverse elongation rate (using 500 μM NTPs) determined from run off

transcription on CKO223 (51 nts) or transcription on CKO223 (23+ nt) (Experimental Procedures and Supplemental Methods) versus α-amanitin concentration using non-linear regression in GraphPad Prism. Values shown are ± standard error as determined by GraphPad Prism.

Supplemental Experimental Procedures

Elongation Complex Formation and Pol II Purification

Yeast Pol II enzymes for biochemistry experiments were purified as were enzymes for nucleotide selectivity experiments in (Wang et al., 2006), via a tandem-affinity epitope tag on the Rpb3 subunit of Pol II (Puig et al., 2001; Wang et al., 2006). In these purifications, the calmodulin affinity resin-binding step was omitted in favor of passing the IgG eluate first through a Hi-Trap SP column (1 mL)(GE Healthcare) followed by buffer exchange into uno-Q buffer (25 mM Tris-Acetate, 65 mM $(NH_4)_2SO_3$, 1 mM EDTA, 5% glycerol, pH 7.9 (4˚ C)) and loading onto an uno-Q ion exchange column (Bio Rad). Pol II containing fractions were eluted by a gradient of $(NH_4)_2SO_4$ and pooled followed by concentration and exchange into *in vitro* transcription (TB) buffer (20 mM Tris pH 8.0, 40 mM KCl, 5 mM $MgCl_2$, 2 mM DTT) plus 5% glycerol. Aliquots of 1 mg/mL were snap-frozen in liquid nitrogen and stored at -80˚C until use.

Pol II elongation complexes for single nucleotide addition experiments were formed with nucleic acid scaffolds as in (Wang et al., 2006) by the method of (Komissarova et al., 2003), save in some experiments half reactions were performed (50% reduction of all quantities in half the volume). For 2'-dNTP and mismatched NTP substrates, incorporation rates could be determined directly from time courses of incubation with

substrate. For single NTP substrates, dilution series of ATP or GTP were used to determine the concentration of substrate that gave half-maximal incorporation over a 5 minute incubation at room temperature as in (Wang et al., 2006).

For elongation rate determination using mixed NTP substrates, an RNA-DNA hybrid was formed by annealing 300 pmol of an 81 nt template oligo, CKO223, with 300 pmol of a 9-mer RNA oligo (RNA9, the same RNA used single nucleotide addition experiments) (end-labeled with γ-^{32}P-ATP using T4 kinase) in 20 µL of in 1X TB (annealing as in (Wang et al., 2006)). 2.5 µL or 5 µL of hybrid were incubated with 5 µg Pol II (5 µL) for 5 minutes at room temperature followed by incubation with 300 pmol of a non-template strand oligo complementary to CKO223 (CKO222) for 5 minutes at room temperature. Complexes were diluted in TB and aliquoted for time course reactions. Active complexes were advanced 1 nt to separate them from excess labeled RNA by addition of GTP to 5 µM for 5 minutes at room temperature (1 µM for E1103G Pol II complexes that have higher affinity for substrates and higher misincorporation rate). Elongation complexes were then mixed with an equal volume of 2X NTP cocktail containing equimolar concentrations of ATP, CTP, GTP and UTP (GE Healthcare) in TB buffer.

Oligonucleotide sequences and schematic of EC scaffolds

Scaffolds for single-nucleotide addition assays

```
                                  +1+2
        RNA9   5'  AUCGAGAGGCA    ctgcttatcggtag 3' Non Temp
ATP Template   3' gtagctctccgtgcagacgaatagccatc 5'

                                  +1+2
        RNA9   5'  AUCGAGAGGAG    ctgcttatcggtag 3' Non Temp
GTP Template   3' gtagctctcctcgcagacgaatagccatc 5'
```

Scaffold for TFIIS cleavage of artificially backtracked complex

```
                                C 3′
                               G
        RNA13   5′  AUCGAGAGGAU   ctgcttatcggtag 3′ Non Temp
UTP Template   3′ gtagctctcctagcagacgaatagccatc 5′
```

RNA oligos in blue, template strand in black, non-template strand in underlined black. For single nucleotide addition assays, complexes are labeled via transcription by incorporation of ^{32}P-α-NMP at position +1 (shown in red), then assayed for addition of either ATP or GTP derivatives at +2 (highlighted).

Scaffold for run off transcription assays, TFIIS cleavage of stalled complexes

```
CKO222 5′ ccatagccttacttacagccatcgagagggacacggcgaaaagccaacccaagcaacaccggggtccgggacgggcaaccc 3′
RNA9   5′                    AUCGAGAGG
CKO223 3′ ggtatcggaatgaatgtcggtagctctccctgtgccgcttttcggttgggttcgttgtggcccca ggccctgcccgttggg 5′
```

CKO223 is the template strand, CKO222 is the non-template, RNA9 (shown in blue) is the initiating 9-mer oligo. For TFIIS cleavage experiments, complexes were allowed to transcribe with ATP, GTP and CTP causing stalling at the template +44 A (underlined, bolded).

TFIIS purification

An RNA-cleavage competent N-terminal truncation of TFIIS (TFIISΔ2-146) was expressed in *E. coli* BL21 (DE3) Codon Plus (Stratagene) from a modified pCR-T7nt-TOPO vector (Invitrogen) and purified via an N-terminal 6-His tag using Ni^{2+}-NTA resin per the manufacturer's instructions (Qiagen). Following imidazole elution of recombinant TFIISΔ2-146 from Ni^{2+}-NTA resin, eluate was precipitated with $(NH_4)_2SO_4$ (0-52.5% cut) and resuspended in TFIISΔ2-146 resuspension buffer (1 μM ZnOAc, 25

mM Tris pH 8, 5% glycerol), aliquoted and stored at 8 mg/mL at -80˚C until use. TFIISΔ2-146 was diluted just before use to 2× concentration, plus or minus 2× α-amanitin and added to an equal volume of stalled Pol II complexes giving a final concentration of 1× TFIISΔ2-146, 1× α-amanitin.

Figure S1. ***In vitro*** **transcription of wild type (WT) and Rpb1 H1085Y Pol II**. A. Quantification of *in vitro* elongation assays for WT and H1085Y Pol II at different concentrations of NTPs. Time courses of *in vitro* transcription were analyzed by denaturing polyacrylamide gel electrophoresis as shown in Figure 2A, exposed to a PhosphorImager screen and quantified by determination of the fraction of signal present in the full-length, 61 nt product versus the signal for all products 10 nt and higher (derived from active elongation complexes). Assays were performed for several concentrations of NTPs and values were plotted in GraphPad Prism, using non-linear regression to curve-fit and determine the half-time for maximal accumulation at each concentration of NTP. Average elongation rate at each NTPs concentration was calculated by dividing the length of transcribed region, 51 nt, by the half-time of maximal accumulation. The fraction of full-length product decreases with decreasing NTP concentration due to the increased amount of Pol II stalling and arrest at lower NTP concentrations. Left panel shows quantification of wild type (WT) Pol II. Right panel shows quantification of H1085Y Pol II. Average elongation rates from multiple experiments calculated in this fashion were in turn plotted versus NTP concentration in GraphPad Prism (Figure 2A), with non-linear regression curve-fitting used to infer maximal average elongate rate. B. Quantification of *in vitro* transcription assays for WT

and H1085Y Pol II at different concentrations of 2'-dATP or 2'-dGTP as shown in Figure 2B. Time courses for single nucleotide addition of different concentrations of either 2'-dATP (top row or panels) or 2'-dGTP (bottom row of panels). Labeled 10 nt RNA products were advanced to 11 nt by addition over a time course of template-specified substrate. Transcripts were separated by denaturing polyacrylamide gel electrophoresis and visualized by PhosphorImager analysis (left panels). The fraction of transcripts that were elongated to 11 nt by addition of 2'-dNTP substrate over time were determined by the ratio of signal at 11 nt divided by combined signal at 10 and 11 nt at each time point and plotted in GraphPad Prism. Plots for 2'-dATP experiments are shown in the top row (WT on left, H1085Y on right) and plots for 2'-dGTP experiments on the bottom row (WT on left, H1085Y on right). Incorporation rate was determined as the reciprocal of the half-time for maximal accumulation inferred from curve-fitting by non-linear regression (the results shown in Figure 2B). For some experiments with low concentrations of 2'-dATP, plots were not adequately curve-fit, due to very inefficient substrate usage. In such cases values were not fit and not used. C. Elongation complexes lose ability to elongate over time. In all of our experiments, more slowly elongating polymerases, whether due to a mutation in Pol II or reduced substrate concentration, gave lower maximal accumulation values, most likely due to increased competition for off-pathway events such as backtracking, arrest or complex dissociation. This phenomenon is especially obvious for very inefficiently used substrates, such as 2'-dNTPs above. This phenomenon is illustrated by preparation of elongation complexes containing a labeled 10 nt transcript as in Figure 2B and above, followed by a time course of incubation at room temperature in the absence of substrate. Complexes were

challenged at various times after preparation with 200 μM ATP for one minute to advance complexes remaining competent to elongate to 11 nt. Representative time courses for WT and H1085Y Pol II are shown in the left panels and experiments from elongation complexes prepared on two different days are plotted in the graphs. D. Quantification of *in vitro* transcription assays for WT and H1085Y misincorporation of GTP. 10 nt labeled RNA-containing elongation complexes prepared as described in Figure 2C and above with a template specifying the addition of ATP at position 11. These complexes were incubated with 1 mM GTP for a time course and transcript products were visualized by PhosphorImager analysis following denaturing polyacrylamide gel electrophoresis. Representative time courses for WT and H1085Y Pol II shown on left. The GTP misincorporation event is readily apparent from any possible ATP contamination of the GTP stock by mobility of the relevant 11-mer products following gel electrophoresis (bottom panel). Fractions of complexes misincorporating GTP over time were plotted for multiple experiments for WT and H1085Y Pol II in the graph on the right. Misincorporation rates shown in Figure 2C were determined as the reciprocal of the half-time of maximal misincorporation to 11 nt as determined by curve-fitting by non-linear regression of values plotted in GraphPad Prism. E. Single nucleotide addition of ATP or GTP by WT or H1085Y Pol II. Pol II ECs prepared and labeled by incorporation as described above on templates specifying either ATP or GTP at position 11 were incubated with a wide range of specified NTP (ATP, left panels, GTP, right panels) for 5 minutes at room temperature. The fraction of complexes that elongated to 11 nt in representative replicate experiments were plotted versus concentration of NTP (ATP, left graph, GTP, right graph).

Supplemental Figure 1

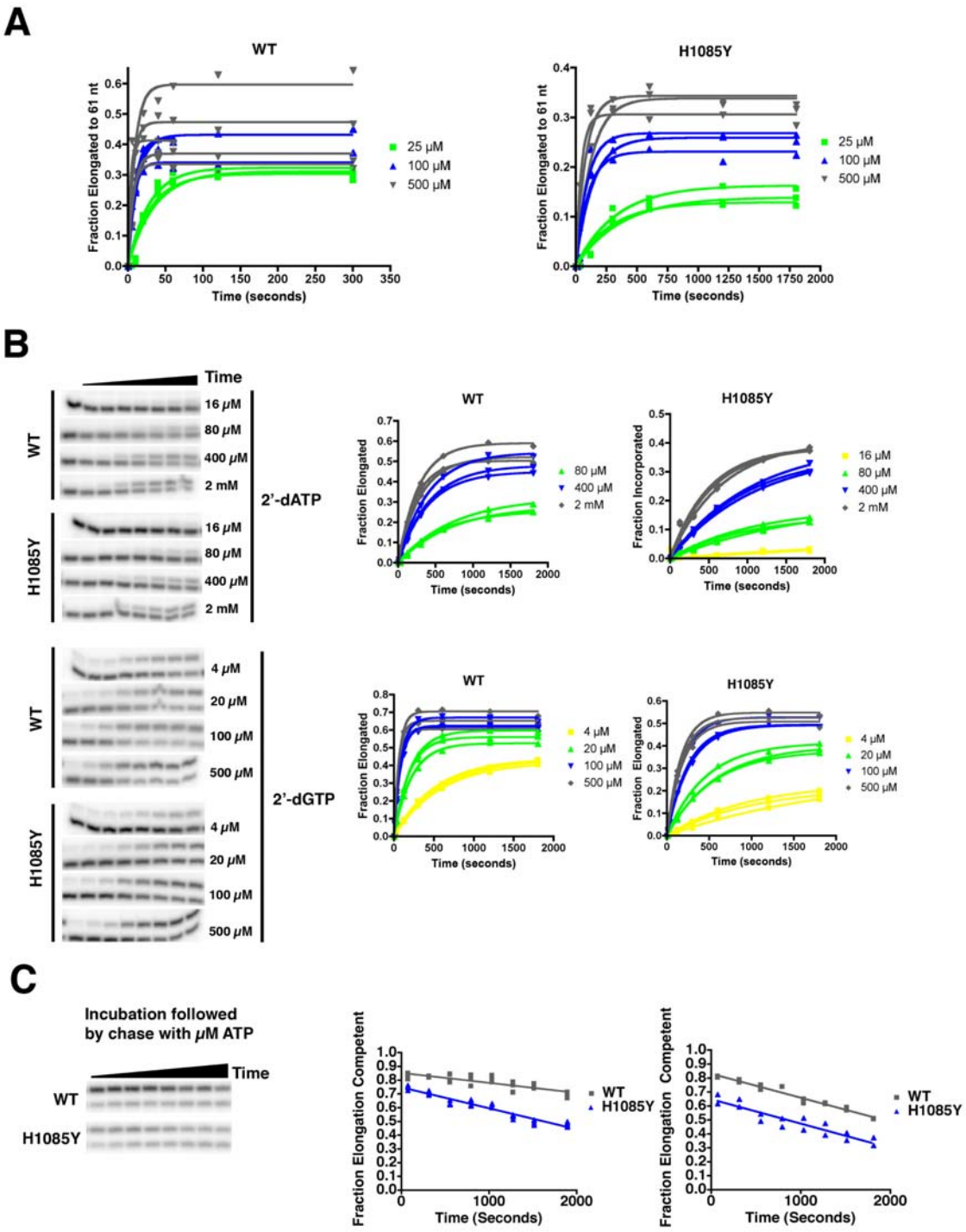

Supplemental Figure 1 (cont)

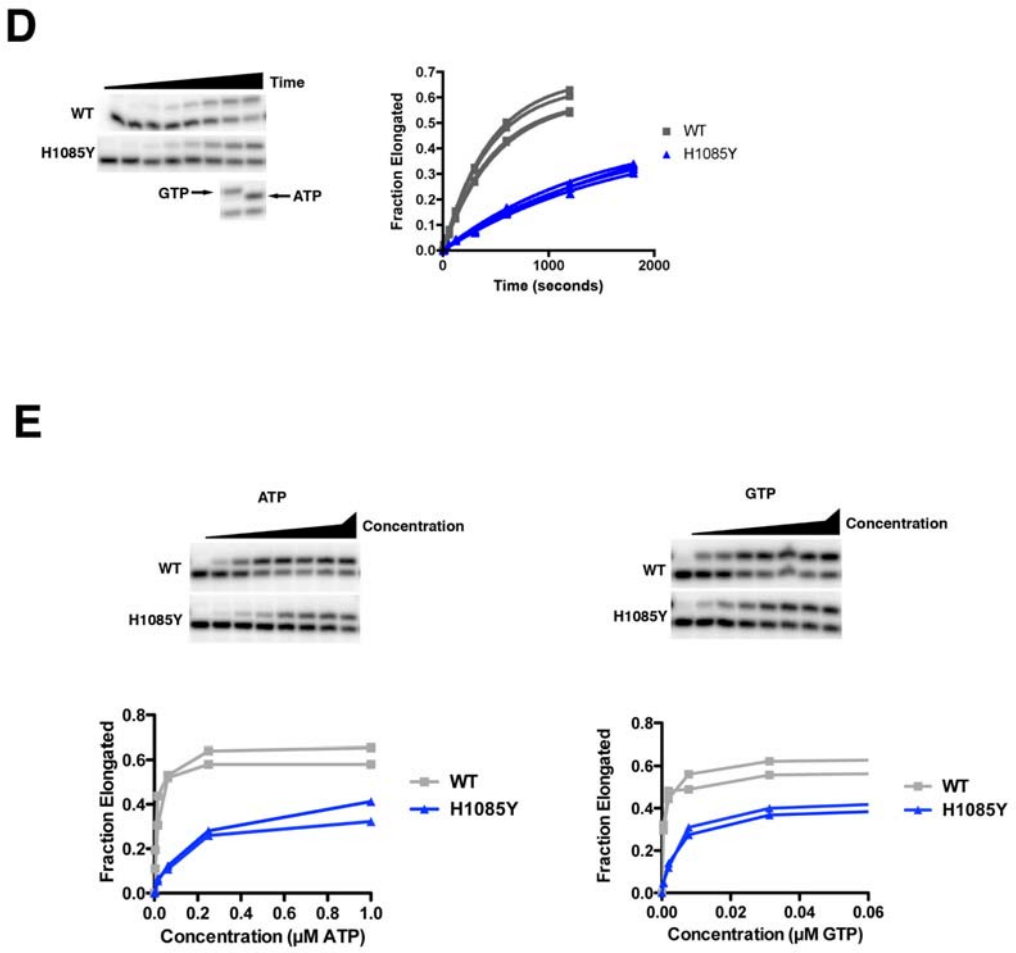

Figure S2. ***In vitro*** **transcription and α-amanitin treated WT and H1085Y Pol II elongation complexes.** A. Quantification of α-amanitin inhibition of elongation by WT and H1085Y Pol II at different concentrations of NTPs. Elongation assays described in

Figure 2A and Supplemental Figure 1A were performed at different concentrations of NTPs for WT and H1085Y in the presence of 40 μg/mL α-amanitin and reactions products were visualized by PhosphorImager analysis following denaturing polyacrylamide electrophoresis (top panels). Fractions of complexes reaching full-length (61 nt) were plotted versus time (left and center graphs) as in Supplemental Figure 1A. Elongation rates calculated from these plots were plotted versus NTP concentration (right graph) to determine maximal elongation rates for WT and H1085Y Pol II in the presence of 40 μg/mL α-amanitin (shown in Figure 3A). Values for α-amanitin-treated WT Pol II using 25 μM NTPs were not used in maximal elongation rate analysis because accumulation was too slow to accurately curve-fit. B. Quantification of α-amanitin inhibition of 2'-dATP or 2'-dGTP incorporation by WT and H1085Y Pol II. Time courses for single nucleotide addition of different concentrations of either 2'dATP (top row or panels) or 2'-dGTP (bottom row of panels). Labeled 10 nt RNA products, pre-incubated with 80 μg/mL α-amanitin were advanced to 11 nt by addition over a time course of template-specified substrate in the presence of 40 μg/mL α-amanitin. Transcripts were separated by denaturing polyacrylamide gel electrophoresis and visualized by PhosphorImager analysis (left panels). The fraction of transcripts that were elongated to 11 nt by addition of 2'-dNTP substrate over time were determined by the ratio of signal at 11 nt divided by combined signal at 10 and 11 nt at each time point and plotted in GraphPad Prism. Plots for 2'-dATP experiments are shown in the top row (WT on left, H1085Y on right) and plots for 2'-dGTP experiments on the bottom row (WT on left, H1085Y on right). Incorporation rate was determined as the reciprocal of the half-time for maximal full-length accumulation inferred from curve fitting by non-

linear regression (the results shown in Figure 3B). For some experiments with low concentrations of 2'-dATP, plots were not adequately curve-fit, due to very inefficient usage. C. Quantification of α-amanitin inhibition of GTP misincorporation by WT or H1085Y Pol II. 10 nt labeled RNA-containing elongation complexes prepared as described in Figure 2C and above with a template specifying the addition of ATP at position 11. These complexes were pre-incubated with 80 μg/mL α-amanitin, following a time course of 1 mM GTP addition in the presence of 40 μg/mL α-amanitin. Reaction products were visualized by PhosphorImager analysis following denaturing polyacrylamide gel electrophoresis. Representative time courses for WT and H1085Y Pol II shown on left. Fractions of complexes misincorporating GTP over time were plotted for multiple experiments for WT and H1085Y Pol II in the graph on the right. Values shown in Figure 3C were calculated from the reciprocal half-times of maximal misincorporation determined by non-linear regression and curve-fitting of the values plotted here.

Supplemental Figure 2

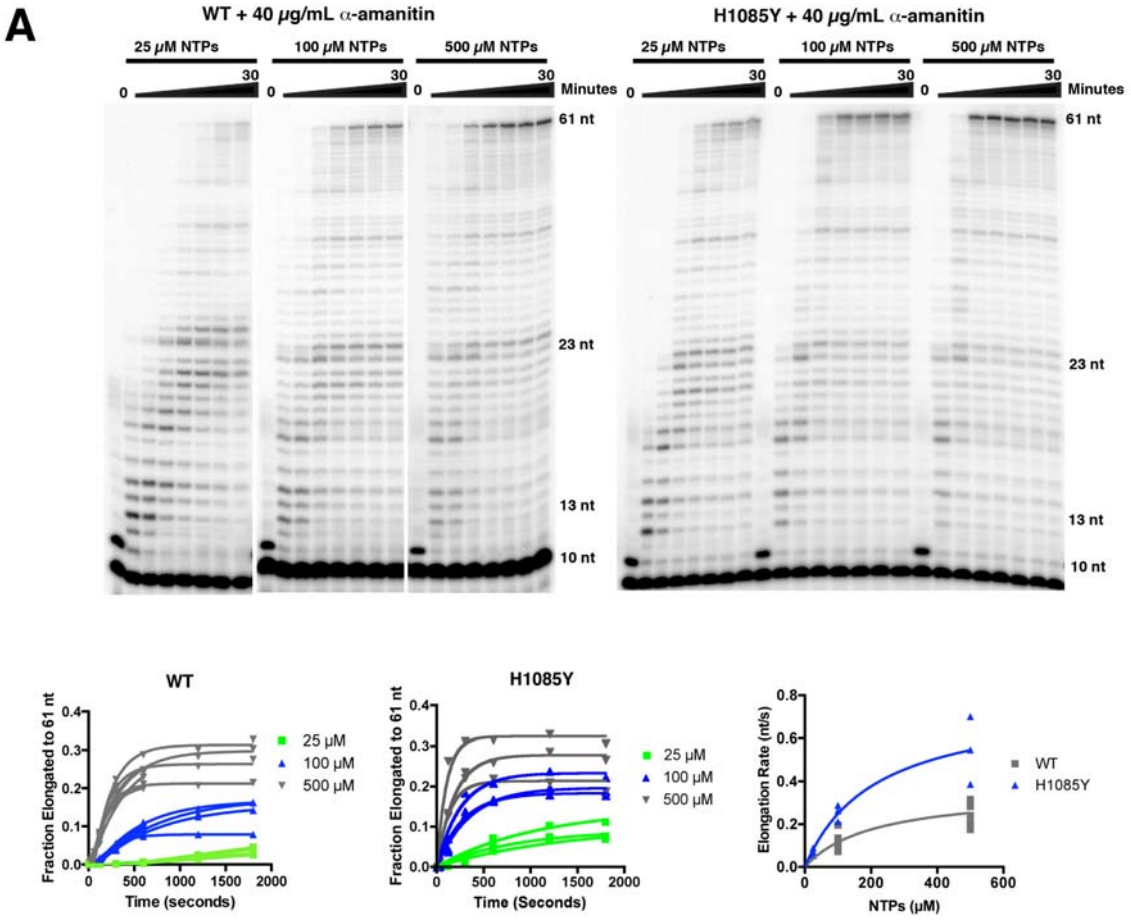

Supplemental Figure 2 (cont)

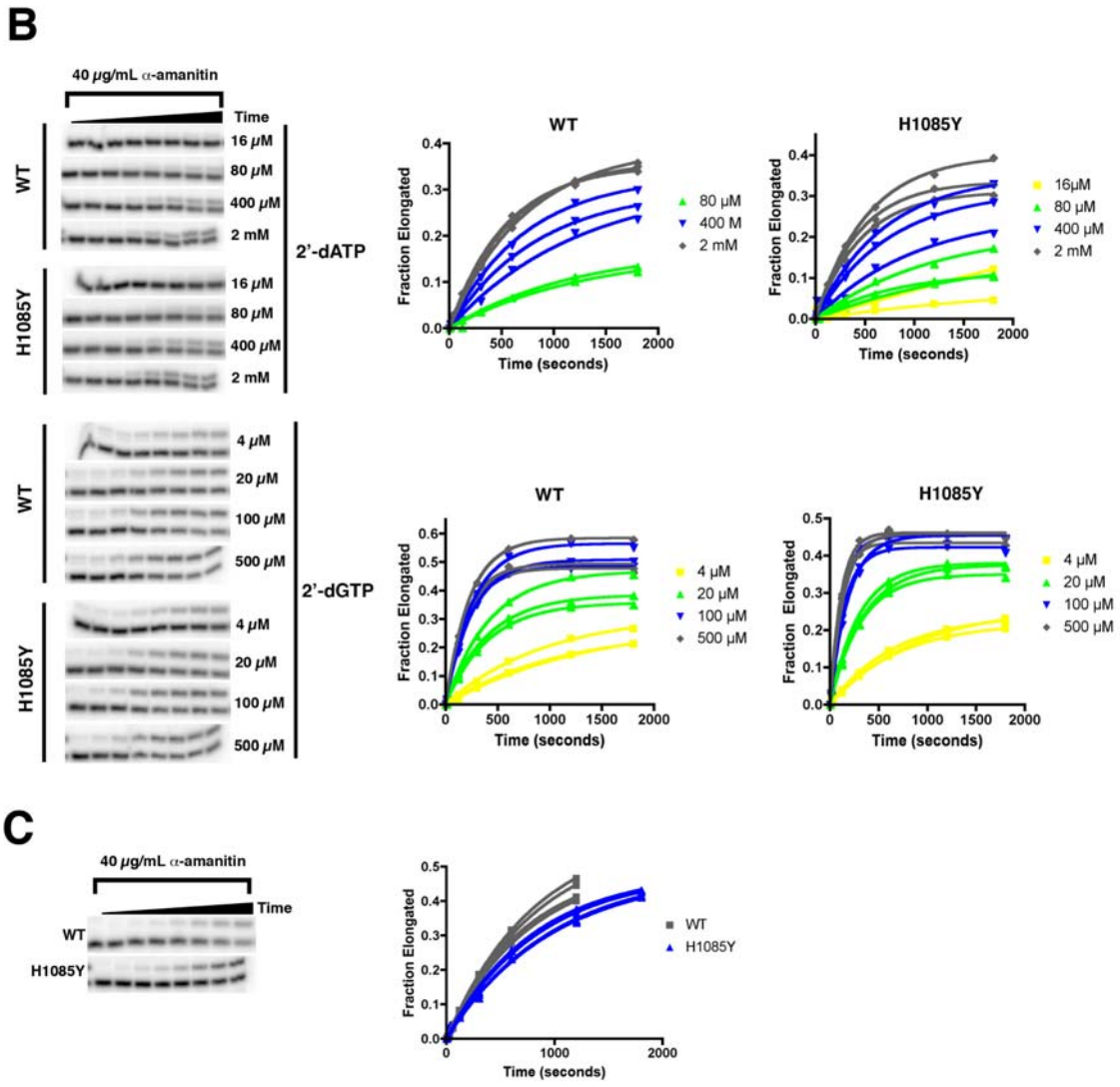

Figure S3. Characterization of TL mutants for *gal10*Δ*56* suppression.

A. In addition to the MPA^{S} and Spt^{-} phenotypes described in the text, we also characterized trigger loop mutants for phenotypes relating to mRNA processing defects and transcriptional interference. The top panel shows the major transcripts present at the wild type *GAL10*-*GAL7* locus in *S. cerevisiae*. In our genetic screens, we sought Pol II mutants able to modulate a phenotype deriving from transcriptional interference at *GAL7*, which occurs when the upstream gene, *GAL10*, has its major polyadenylation signal compromised by a small deletion (*gal10*Δ*56*)(bottom panel), allowing transcription originating from *GAL10* to read into *GAL7*. This read-through transcription inhibits *GAL7* production rendering cells sensitive to galactose (Gal^{S}). Pol II mutants, Pol II elongation factor mutants, mRNA processing and mRNA export mutants modulate the intensity of this phenotype (Bucheli et al., 2007; Bucheli and Buratowski, 2005; Greger et al., 2000; Greger and Proudfoot, 1998; Kaplan et al., 2005). B. 10-fold serial dilutions of TL mutant saturated liquid cultures were spotted on YP Raffinose plates (rich media supplemented with 2% Raffinose) as a control or YP Raffinose/Galactose plates (rich media supplemented with 2% Raffinose and 1% Galactose) to assay the Gal^{S} phenotype induced by *gal10*Δ*56*. We identified several TL alleles able to suppress *gal10*Δ*56* in a plate assay and one TL mutant, F1084I, able to enhance it.

Supplemental Figure 3

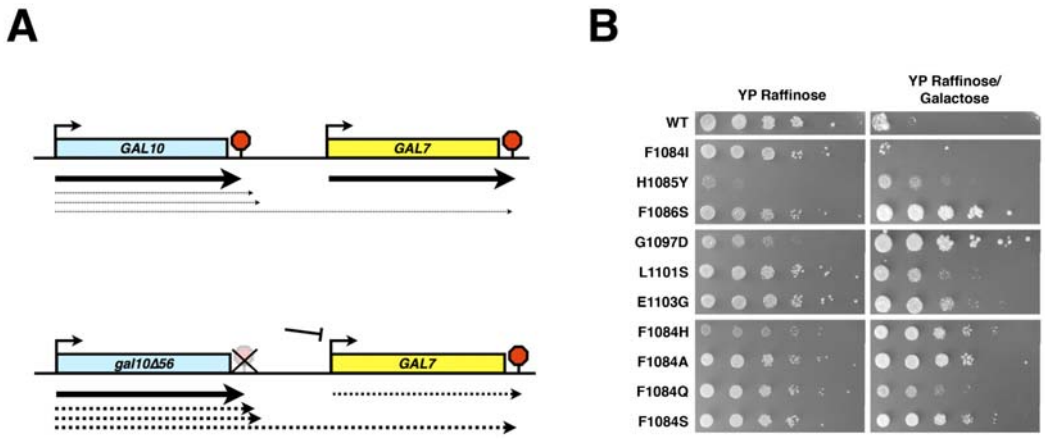

Figure S4. Pol II TL mutant inhibition by α-amanitin and substrate-selective effects on *in vitro* transcription. A. Quantification of Pol II TL mutant elongation rates and effects of 40 μg/mL α-amanitin. The elongation assay as described in Figure 2A, 3A, and Supplemental Figures 1A and 2A was performed for a number of Pol II TL mutants. *Top row, left*: Untreated (no drug) full-length transcript (61 nt) accumulation for F1084I Pol II at a number of NTP concentrations for multiple experiments plotted versus time of incubation. *Top row, center:* 40 μg/mL α-amanitin treated 61 nt transcript accumulation for F1084I Pol II at a number of NTP concentrations for multiple experiments plotted versus incubation time. *Top row, right*: F1084I elongation rates determined from graphs on left and center plotted versus NTP concentration (note logarithmic scale). *Middle row, left:* Untreated (no drug) full-length transcript (61 nt) accumulation for F1086S Pol II at a number of NTP concentrations for multiple experiments plotted versus time of incubation. *Middle row, center:* 40 μg/mL α-amanitin treated 23 nt transcript accumulation for F1086S Pol II at a number of NTP concentrations for multiple experiments plotted versus incubation time. Note that elongation causes sufficient slowing of Pol II such that elongation to 23 nt and above is quantified instead of full length (61 nt) transcript. Average elongation rates are generally faster for shorter products because fewer positions are available where pausing on the timescale of the experiment can contribute to the accumulation of specified product. An exception to this trend would be for very short products that happen to include a strong pause site subsequent to production of the specified transcript length. In such a case the rate of pause escape would dominate the rate of accumulation of any larger products. For the template used here, there is a major pause site at 23 nt. *Middle row, right*: F1086S

elongation rates determined from graphs on left and center plotted versus NTP concentration (note logarithmic scale). *Bottom row, left:* Untreated (no drug) full-length transcript accumulation (61 nt) for E1103G Pol II at a number of NTP concentrations for multiple experiments plotted versus time of incubation. *Bottom row, center:* 40 μg/mL α-amanitin treated full-length transcript accumulation (61 nt) for E1103G Pol II at a number of NTP concentrations for multiple experiments plotted versus incubation time. *Bottom row, right*: E1103G elongation rates determined from graphs on left and center plotted versus NTP concentration (note logarithmic scale). B. Quantification of Pol II TL mutants 2'-dGTP addition rates and effect of 40 μg/mL α-amanitin. The single nucleotide addition assay as described in Figure 2B, 3B, and Supplementary Figures 1B and 2B was performed for a number of Pol II TL mutants. *Top row, left:* Elongation by F1084I Pol II with different concentrations of 2'-dGTP versus time. *Top row, center:* Elongation by F1084I Pol II with different concentrations of 2'-dGTP versus time in the presence of 40 μg/mL α-amanitin. *Top row, right:* F1084I Pol II 2'-dGTP incorporation rates calculated from the reciprocal half-times for accumulation determined from left and center graphs plotted versus 2'-dGTP concentration. *Middle row, left:* Elongation by F1086S Pol II with different concentrations of 2'-dGTP versus time. *Middle row, center:* Elongation by F1086S Pol II with different concentrations of 2'-dGTP versus time in the presence of 40 μg/mL α-amanitin. *Middle row, right:* F1086S Pol II 2'-dGTP incorporation rates calculated from the reciprocal half-times for accumulation determined from left and center graphs plotted versus 2'-dGTP concentration. *Bottom row, left:* Elongation by E1103G Pol II with different concentrations of 2'-dGTP versus time. *Bottom row, center:* Elongation by E1103G Pol II with different concentrations of 2'-

dGTP versus time in the presence of 40 μg/mL α-amanitin. *Bottom row, right:* E1103G Pol II 2'-dGTP incorporation rates calculated from the reciprocal half-times for accumulation determined from left and center graphs plotted versus 2'-dGTP concentration. C. GTP Misincorporation by Pol II TL mutants and effect of α-amanitin. GTP misincorporation assay was performed for Pol II TL mutants exactly as in Figure 2C, Figure 3C, Supplemental Figures 1C and 2C. *Left:* Misincorporation of GTP by F1084I Pol II in the presence or absence of 40 μg/mL α-amanitin plotted versus time for multiple experiments. *Center:* Misincorporation of GTP by F1086S Pol II in the presence or absence of 40 μg/mL α-amanitin plotted versus time for multiple experiments. *Right:* Misincorporation of GTP by E1103G Pol II in the presence or absence of 40 μg/mL α-amanitin plotted versus time for multiple experiments.

Supplemental Figure 4

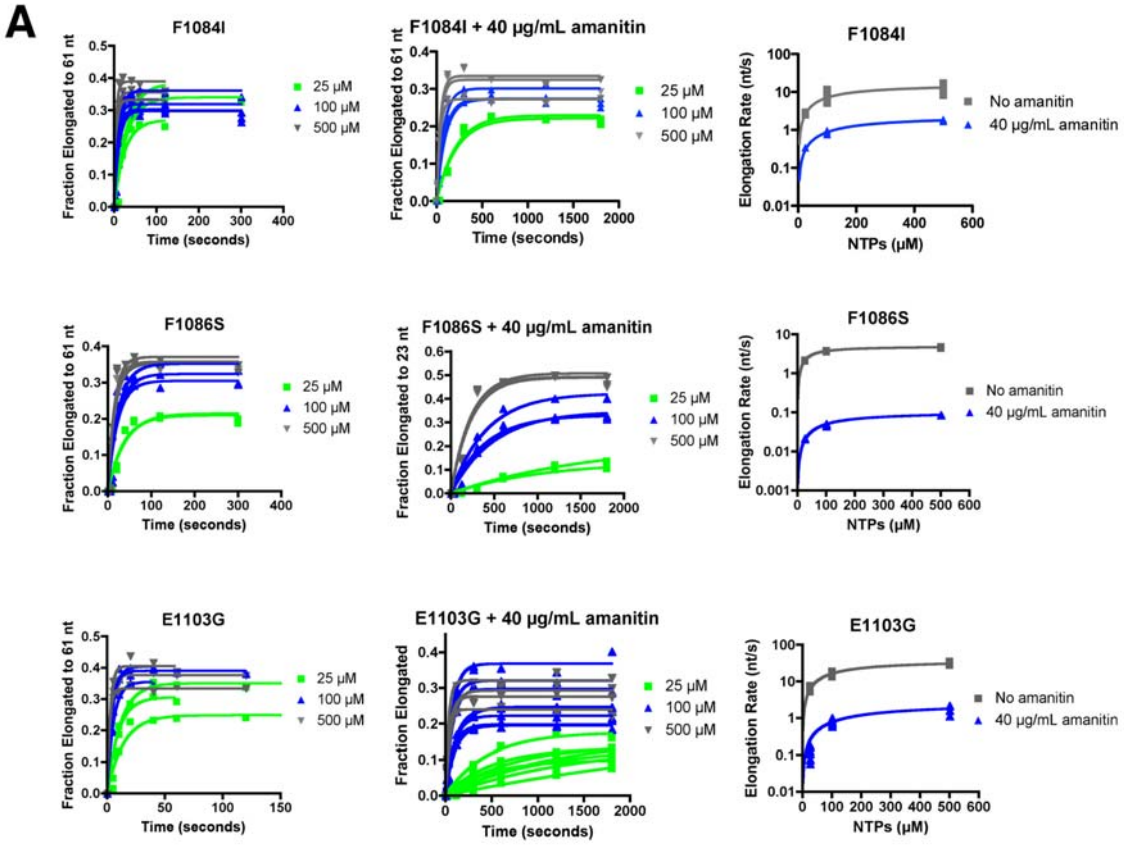

Supplemental Figure 4 (cont)

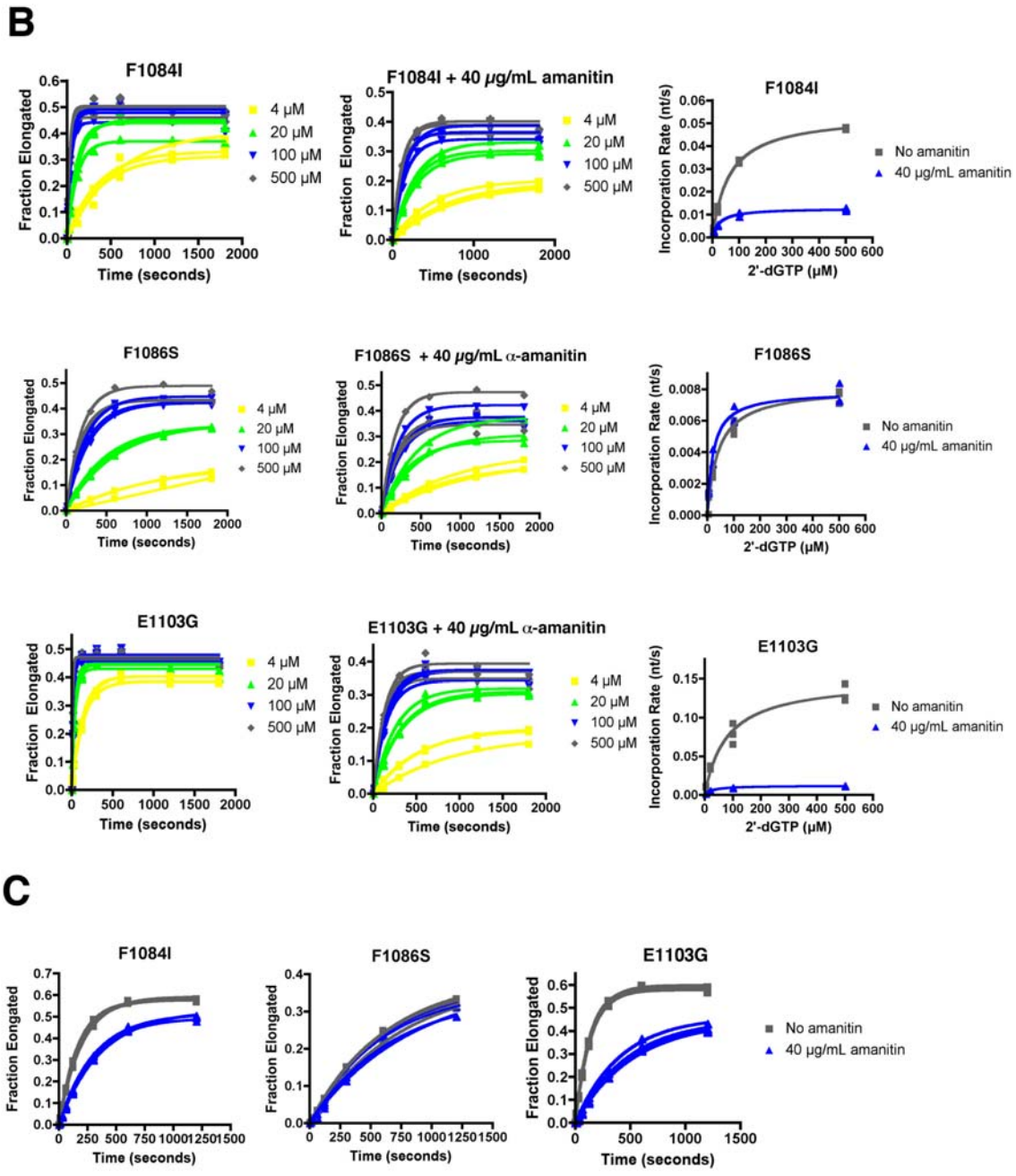

Figure S5. Quantification of α-amanitin and substrate-specific effects on *in vitro* transcription by Calf Thymus Pol II. A. Elongation experiments with NTP substrates and Calf Thymus Pol II were performed exactly as described in Figure 2A, 3A, and Supplemental Figures 1A, 2A, and 3A. Time courses of Calf Thymus Pol II elongation in the presence of different concentrations of NTP without α-amanitin (left panel) or in the presence of 10 μg/mL α-amanitin (center panel). *Top right graph:* Untreated (no drug) full-length transcript (58 nt and above) accumulation by Calf Thymus Pol II at a number of NTP concentrations for multiple experiments plotted versus time of incubation. *Middle right graph:* 10 μg/mL α-amanitin treated Calf Thymus Pol II 13 nt transcript accumulation at a number of NTP concentrations for multiple experiments plotted versus incubation time. *Bottom right graph:* Elongation rates determined from graphs above plotted versus NTP concentration (note logarithmic scale). Elongation rates are slow in all conditions because experiments were performed at room temperature and not the more optimal 37˚C. B. Quantification of Calf Thymus Pol II incorporation 2'-dATP and 2'-dGTP and inhibition by α-amanitin. Calf Thymus Pol II elongation complexes containing a labeled 10 nt RNA were formed as described for all other enzymes in Figures 2B, 3B and Supplemental Figures 1B and 2B. *Top left panels:* Time courses of addition of 2 mM 2'-dATP in the absence of α-amanitin (top) or presence of 10 μg/mL α-amanitin (bottom). *Top center panels:* Addition of 2'-dGTP by Calf Thymus Pol II in the absence of α-amanitin (left) or presence of 10 μg/mL α-amanitin (right). *Top right graph:* Quantification of 2'-dATP addition by Calf Thymus Pol II from multiple experiments. *Bottom left graph:* Quantification of 2'-dGTP addition by Calf thymus (no α-amanitin) from multiple experiments. *Bottom center graph:*

Quantification of 2'-dGTP addition by Calf thymus in the presence of 10 μg/mL α-amanitin from multiple experiments. *Bottom right graph:* 2'-dGTP incorporation rates determined from bottom center and right graphs for Calf Thymus Pol II plotted versus 2'-dGTP concentration. C. Single nucleotide addition of ATP or GTP by Calf Thymus Pol II and α-amanitin inhibition. Calf Thymus Pol II elongation complexes prepared as described above with a labeled 10-mer RNA and templates specifying either ATP or GTP at position 11 were incubated with a wide range of specified NTP (ATP, top panels, GTP, bottom panels) for 5 minutes at room temperature, without α-amanitin treatment (left panels) or with 40 μg/mL α-amanitin (right panels). The fraction of complexes that elongated to 11 nt were plotted versus concentration of NTP (ATP, top graph, GTP, bottom graph). The data were fitted to curves by non-linear regression and the concentrations of ATP or GTP giving half-maximal incorporation under each condition were determined (shown in Figure 5E).

Supplemental Figure 5

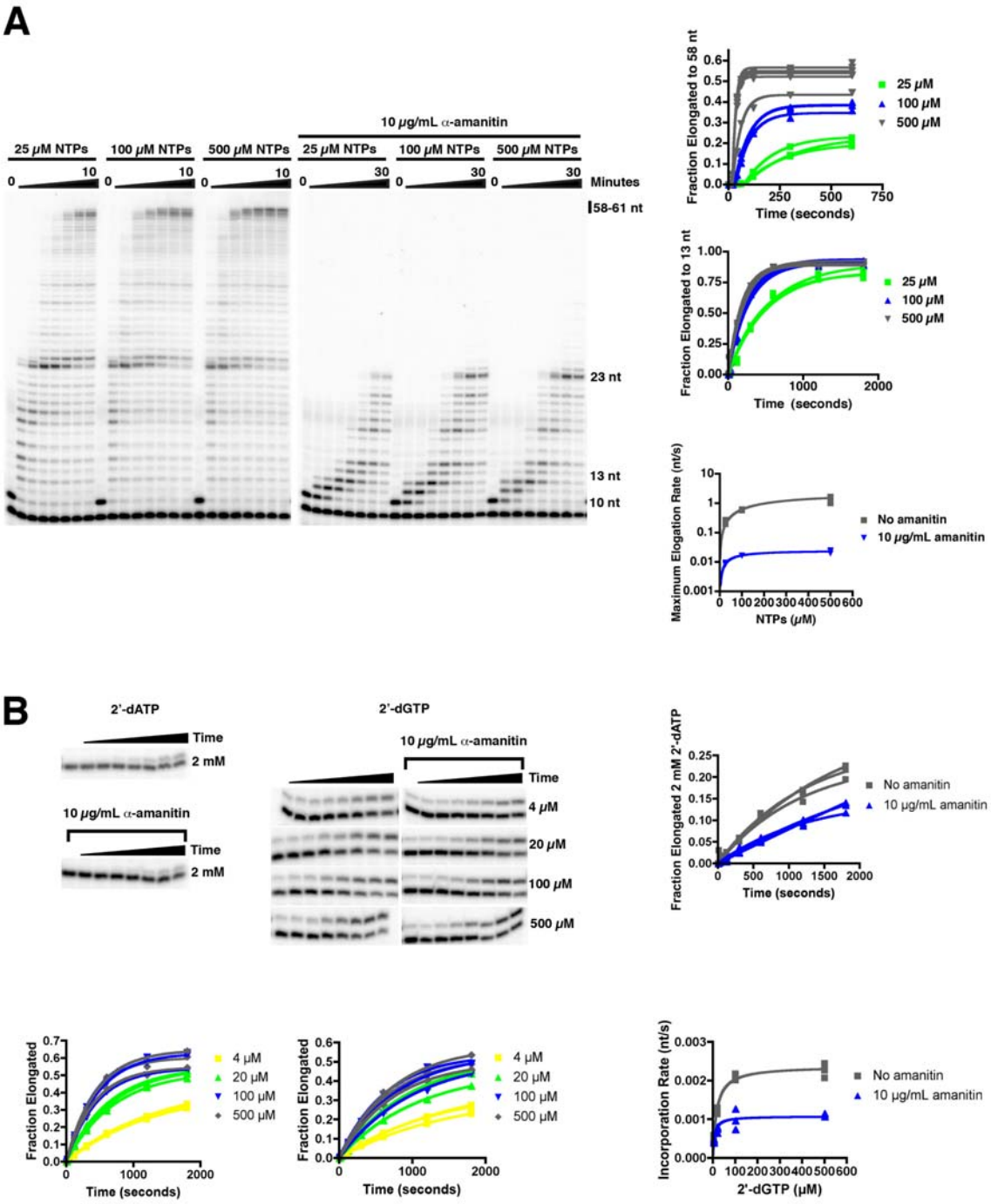

C

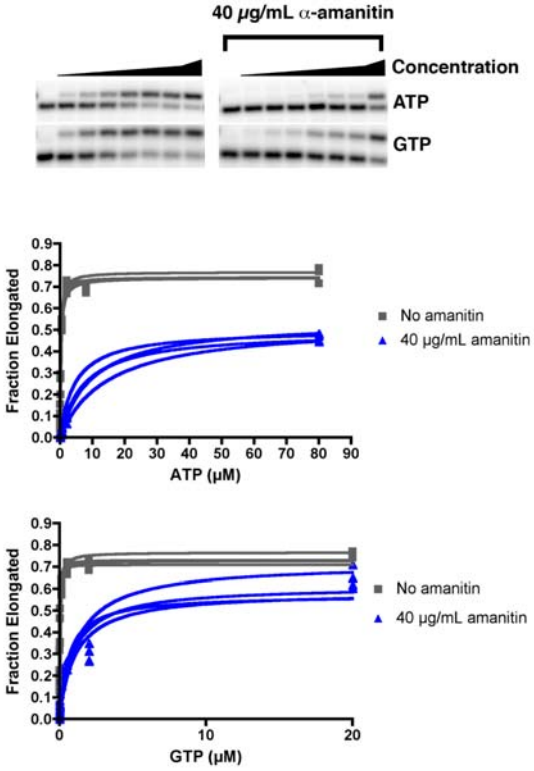
40 μg/mL α-amanitin
Concentration
ATP
GTP
Fraction Elongated
ATP (μM)
No amanitin
40 μg/mL amanitin
Fraction Elongated
GTP (μM)
No amanitin
40 μg/mL amanitin

Supplemental References

Bucheli, M., He, X., Kaplan, C., Moore, C., and Buratowski, S. (2007). Polyadenylation site choice in yeast is affected by competition between Npl3 and polyadenylation factor CFI. RNA.

Bucheli, M. E., and Buratowski, S. (2005). Npl3 is an antagonist of mRNA 3' end formation by RNA polymerase II. Embo J *24*, 2150-2160.

Greger, I. H., Aranda, A., and Proudfoot, N. (2000). Balancing transcriptional interference and initiation on the GAL7 promoter of Saccharomyces cerevisiae. Proc Natl Acad Sci U S A *97*, 8415-8420.

Greger, I. H., and Proudfoot, N. J. (1998). Poly(A) signals control both transcriptional termination and initiation between the tandem GAL10 and GAL7 genes of Saccharomyces cerevisiae. Embo J *17*, 4771-4779.

Kaplan, C. D., Holland, M. J., and Winston, F. (2005). Interaction between transcription elongation factors and mRNA 3'-end formation at the Saccharomyces cerevisiae GAL10-GAL7 locus. J Biol Chem *280*, 913-922.

Komissarova, N., Kireeva, M. L., Becker, J., Sidorenkov, I., and Kashlev, M. (2003). Engineering of elongation complexes of bacterial and yeast RNA polymerases. Methods Enzymol *371*, 233-251.

Puig, O., Caspary, F., Rigaut, G., Rutz, B., Bouveret, E., Bragado-Nilsson, E., Wilm, M., and Seraphin, B. (2001). The tandem affinity purification (TAP) method: a general procedure of protein complex purification. Methods *24*, 218-229.

Vassylyev, D. G., Vassylyeva, M. N., Zhang, J., Palangat, M., Artsimovitch, I., and Landick, R. (2007). Structural basis for substrate loading in bacterial RNA polymerase. Nature *448*, 163-168.

Wang, D., Bushnell, D., Westover, K., Kaplan, C., and Kornberg, R. (2006). Structural basis of transcription: role of the trigger loop in substrate specificity and catalysis. Cell *127*, 941-954.